ADVANCED MATERIALS

Communications

Real-Time Observation of Temperature Rise and Thermal Breakdown Processes in Organic LEDs Using an IR Imaging and Analysis System**

By *Xiang Zhou*, *Jun He*, *Liang S. Liao*, *Ming Lu*, *Xun M. Ding*, *Xiao Y. Hou*,* *Xiao M. Zhang*, *Xiao Q. He*, and *Shuit T. Lee*

Organic light-emitting diodes (OLEDs) hold great promise for future use as large-area flat-panel displays.[1,2] The efficiency, drive voltage, and color selection of the devices reached the standards for commercialization soon after the work reported by Tang and VanSlyke,[1] but the device lifetimes have remained short compared with commercial inorganic semiconductor light-emitting devices. Groups such as Kodak,[2] Uniax, CDT, and Philips have recently reported lifetimes of several tens of thousands of hours.[3] However, the average lifetimes for many groups are below 2000 h. Consequently, an understanding of the degradation mechanisms of OLEDs is of broad interest.[1–29] A lifetime reduction of one or two orders of magnitude has generally been found for OLEDs operated at 60–70 °C compared with room temperature.[2] It is obvious that the lifetimes of OLEDs are limited by their poor thermal stability, so improvement in the thermal stability of OLEDs is essential for progress in their practical applications.[2–15] In particular, electrically pumped lasing from organic-based devices is more susceptible to Joule heating problems because of the existence of unavoidably large current densities.[6,7]

The green-emitting OLEDs consisting of a heterostructure of *N,N′*-diphenyl-*N,N′*-bis(3-methylphenyl)-1,1′-biphenyl-4,4′-diamine (TPD) and tris(8-quinolinolato) aluminum (Alq_3), have been widely investigated.[1–5,8–19,29] Although the microscopic origin of failure remains unclear, a number of studies suggest that failure of these OLEDs may be associated with thermal degradation of the hole-transport layer, the TPD, which has a low glass-transition temperature. Crystallization and intermixing of organic layers have been observed.[8–19] However, the relation of these events to device degradation remains undefined. At this time there is very little published work on the mechanism of thermally activated degradation pathways.[5] Therefore, in-situ temperature measurements on working OLEDs are important for understanding the process of thermal breakdown in the devices.[16]

Short-circuiting is a very common problem during the operation of OLEDs, which results in thermal breakdown and a catastrophic failure of the devices.[2,4,8–10,16] The abrupt cessation of light emission is accompanied by a sharp increase in current density and bursting of the metal film above the damaged spots, which are indicators of the locations of the electrical short.[2–5,8–12,22] It is difficult to determine the location of the electrical short in a failing OLED during operation because light will still be emitted through the ITO glass even after the electrical short has already occurred. In the present work, real-time temperature and radiant power measurements were carried out using an infrared image and analysis system in order to find the electrical shorts as quickly as possible and investigate the thermally-activated degradation process. The positions of electrical shorts were determined easily and quickly. The surface temperature at the site of the electrical short is as high as 86 °C and the temperature inside actual devices can be even higher. The mechanisms responsible for the formation and development of the electrical shorts, and ultimately the catastrophic failure of the OLEDs, are proposed and discussed. Such processes may mainly include the decomposition of ITO and the electromigration of indium at locations of non-planarity.

In the present work, standard quality and fully oxidized indium tin oxide (ITO) coated glass was used as the substrate material. The ITO film was 25 nm thick and had a sheet resistance of 77 Ω/□. The glass substrate was 0.5 mm thick and had 85 % transmittance in the visible range. Moreover, the glass had good heat conductivity and a window at 2.5–4 μm (>60 %) in the IR range because of its thickness. In fact, this ITO glass substrate does not affect the measurement of temperature significantly. For the deposition of organic films, the ITO substrates were kept at room temperature under a pressure of 10^{-5} torr. A 40 nm thick TPD layer was deposited, followed by a 40 nm thick layer of Alq_3. The typical deposition rates of the organic films were 0.2–0.3 nm/s, as measured by a quartz crystal microbalance. Finally, an aluminum cathode electrode was deposited on top of the organic films. The measurement and testing of the ITO/TPD(40 nm)/Alq_3(40 nm)/Al devices

[*] Prof. X. Y. Hou, Dr. X. Zhou, Dr. J. He, Prof. L. S. Liao, Dr. M. Lu, Prof. X. M. Ding
Surface Physics Laboratory (National Key Laboratory)
Fudan University
Shanghai 200433 (China)
Dr. X. M. Zhang, Dr. X. Q. He
National Key Laboratory for Reliability Physics and Application Technology
PO Box 1501-05 Guangzhou 510610 (China)
Prof. S. T. Lee
Department of Physics and Material Science, City University
Hong Kong (China)

[**] The authors would like to thank Prof. Tao and Prof. Zhou for synthesizing the organic materials needed for this research. This work was supported by the NSF of China with grants no. 59832100 and 69776034.

  0935-9648/00/0402-0265 $ 17.50+.50/0

were carried out in air using fresh samples without encapsulation. TPD and Alq_3, the organic materials used in this study, were synthesized in the chemistry department at Fudan University.

Figure 1 shows the forward-bias voltage–current–brightness characteristics of devices and is typical of the *V–I–B*

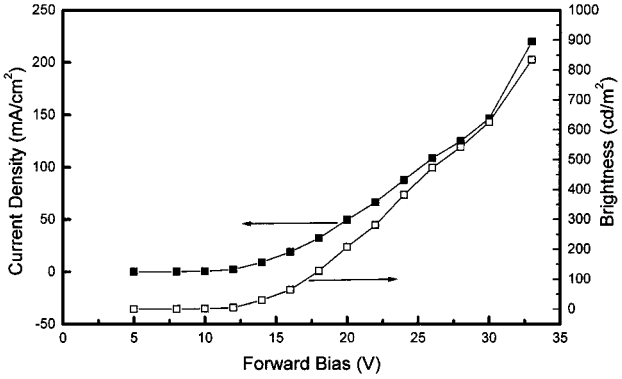

Fig. 1. The *V–I–B* characteristics of the OLEDs.

data obtained from a group of sample OLEDs. When the forward bias exceeds 8 V, light emission can be clearly observed by the naked eye in a natural daylight environment. The luminance of the device is 130 cd/m^2 at 18 V with a current density of 32 mA/cm^2. The luminance increases to 626 cd/m^2 at 30 V with a current density of 146.5 mA/cm^2. The light output is proportional to the current density, which is the same as the results reported in previous work.[1,2,29] We have analyzed systematically the lifetimes of a population of OLEDs under constant voltage in air. We note that under low voltage stress (<18 V), the OLEDs have longer lifetimes and can typically survive for several tens of hours without thermal breakdown, the degradation of the OLEDs in this regime is mainly caused by the formation and propagation of black spots.[1,2,4,8,9,16,19] Under high-voltage stress (>25 V, or high electrical field >3×10^6 V/cm = 24 V/80 nm), OLEDs have short lifetimes of several tens of minutes. Electroluminescence intensity of OLEDs decreases more rapidly and very large leakage currents always form prior to thermal breakdown and catastrophic failure.[4,8,10–16,22] It is obvious that the thermal degradation of OLEDs is significant under high-voltage stress.

Real-time measurements of the temperature of the OLEDs operating under a constant voltage were carried out with an InfraScope infrared imaging and analysis system made by EDO Corporation. A schematic diagram of the experimental set-up is shown in Figure 2. An OLED sample is placed at the focal point of the objective lens of the infrared imaging system. In order to calibrate the surface temperature of a sample, the emissivity of the sample and the ambient radiance must be determined by measurements of the radiance of the sample at two given temperatures. The two temperatures chosen for the calibration of temperature measurements are obtained by heating the sample externally and uniformly in the test stand. Then the

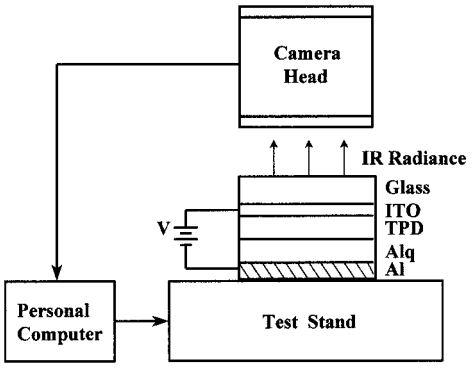

Fig. 2. Experimental set-up used for measurement of temperature.

drive voltage was applied to the OLED and the test stand kept at 29 °C by a heater controller as a fixed background temperature. The temperature images of the surface of the working OLED can be obtained after applying voltage for 20 s. The infrared radiance produced inside the working OLED passes through the ITO glass and is detected by the infrared camera head of the InfraScope system. The actual temperature of the surface is determined from the measurements of the radiance (mW/cm^2-steradian) of the sample. The surface morphologies of OLEDs after thermal breakdown were studied using a Philips XL-30 FEG SEM and 4i-EDAX system.

Figure 3 demonstrates a typical surface temperature image sequence of a working OLED. The active area of the OLED, which is defined by the overlap of the ITO (6 mm wide) and Al stripes (3 mm wide) as marked by the solid lines, is about 3×6 mm^2 At a forward bias of 18 V and a current density of 32 mA/cm^2, a significant temperature difference between the active area and the outside area (background) appears, as shown in Figure 3a. The highest temperature in the active region is about 35 °C. The temperature in the center of the device is higher than that in the region close to the edges because of heat dissipation. The highest temperature of the OLED as a function of the forward bias is plotted in Figure 4. This temperature–voltage (*T–V*) curve has two regions. In the low-forward-bias region (<28 V), the temperature increases linearly with increasing voltage. The temperature images in this region show strong uniformity in the light-emitting area as shown in Figure 3a to Figure 3e. At a forward bias of 28 V, the temperature image, as shown in Figure 3f, begins to show a non-uniform feature because the temperature in the area near the right edge of the OLED is higher than that in the remainder. In the high-forward-bias (>28 V) region, the non-uniformity of the temperature is obviously seen in Figure 3g and Figure 3h. The temperature is not linearly related to the forward bias. The *T–V* curve no longer satisfies the linear relation in the high-forward-bias regime. The "hot-spot" near the right edge of the OLED is very clearly observed in Figure 3h, which indicates the formation of an electrical short in the OLED. The hot-spot is elliptical in shape because the heat dissipation along the aluminum

0935-9648/00/0402-0266 $ 17.50+.50/0

ADVANCED MATERIALS

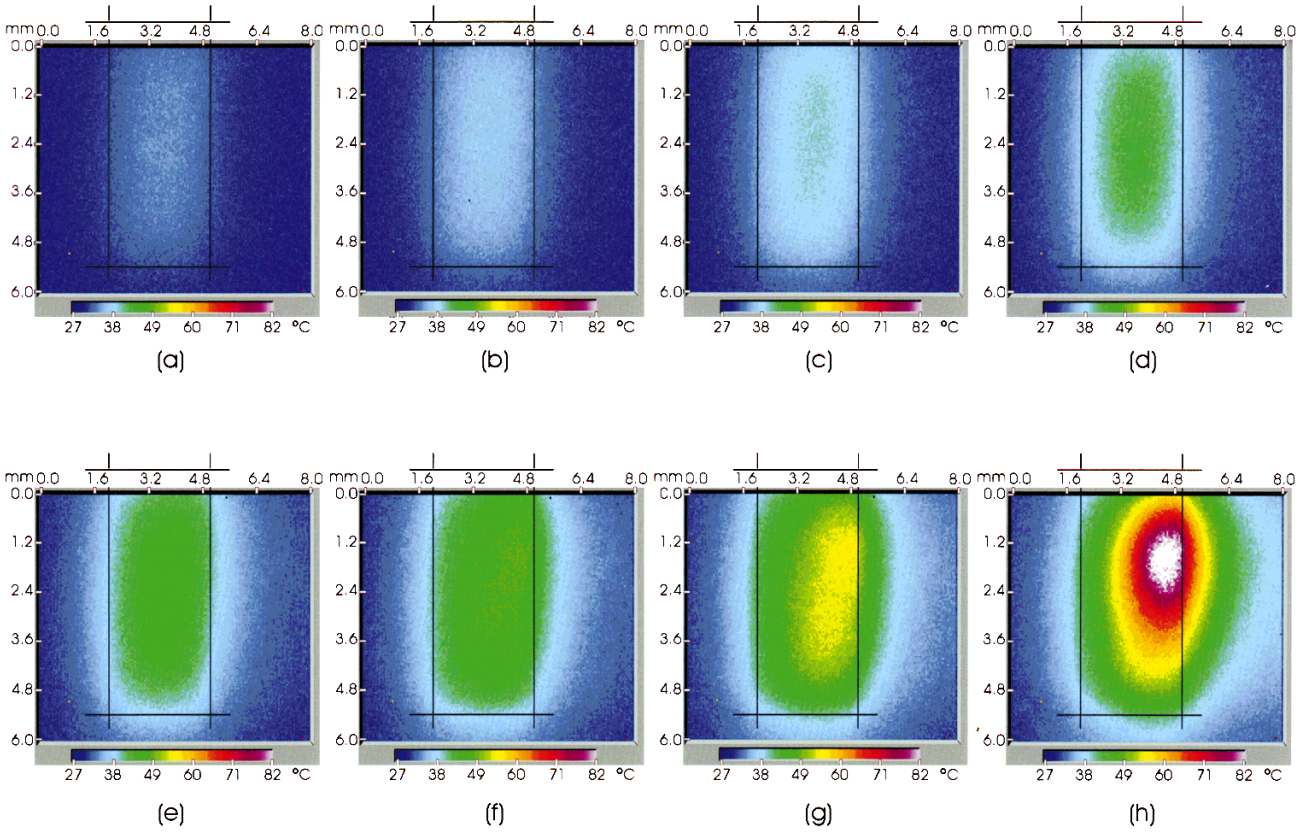

Fig. 3. Surface temperature images of OLEDs: a) 18 V, 32 mA/cm^2, 35 °C; b) 20 V, 49 mA/cm^2, 37 °C; c) 22 V, 66.5 mA/cm^2, 40 °C; d) 24 V, 87.7 mA/cm^2, 43 °C; e) 26 V, 108 mA/cm^2, 46 °C; f) 28 V, 125 mA/cm^2, 49 °C; g) 30 V, 146.5 mA/cm^2, 55 °C; h) 33 V, 220 mA/cm^2, 86 °C.

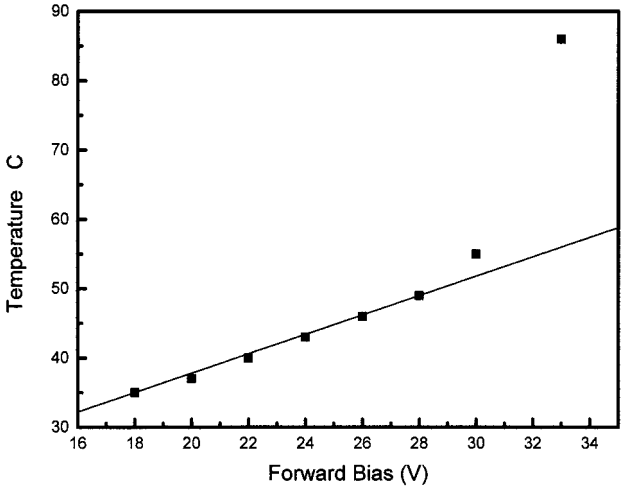

Fig. 4. Highest temperature in the Al/Alq_3/TPD/ITO device as a function of the forward bias.

stripe is faster than that in the orthogonal direction. The exact position and diameter of the electrical short can not be precisely determined from the temperature image because of the heat dissipation. The average diameter of hot-spot is measured to be about 0.86 mm from Figure 3h. At the start of the formation of an electrical short, as in Figure 3g, the temperature deviates slightly from the linear pattern, as shown in Figure 4, while intense light emission can be observed. Because of the low impedance in the short, a very large current flows through the electrical short and the current in the remainder of the device is reduced dramatically. Thus the short sustains a very large current and the temperature at this position is subsequently raised as result of Joule heating. The surface temperature at the center of the hot-spot reaches 86 °C, as shown in Figure 3h. In fact, the temperature inside actual devices can be even higher. The glass transition temperature, T_g, of the TPD in the device is only 60 °C.[13–15,17,18] At a temperature above T_g, the TPD layer tends to crystallize and the morphology change causes an electrical inhomogeneity in the OLED.[17,18] For this reason, TPD has now largely been replaced by *N*,*N*′-di(naphthalene-1-yl)-*N*,*N*′-diphenyl-benzidine (NPB) with T_g = 110 °C in vacuum deposited OLEDs with improved stability.[13] Tokito et al.[10–12] have shown that a tetramer of triphenylamine (TPTE) with T_g = 130 °C can also be used as an efficient hole-transporting material. Such TPTE/Alq_3-based devices were demonstrated to have stable operation at $T<T_g$, indeed, storage at T = 150 °C was not found to result in significant degradation of the device characteristics when operated after returning to room temperature.

Figure 5 is an SEM image showing the morphology of the top Al electrode of the OLEDs after thermal breakdown. The surface of the Al electrode is corrugated as a

  0935-9648/00/0402-0267 $ 17.50+.50/0

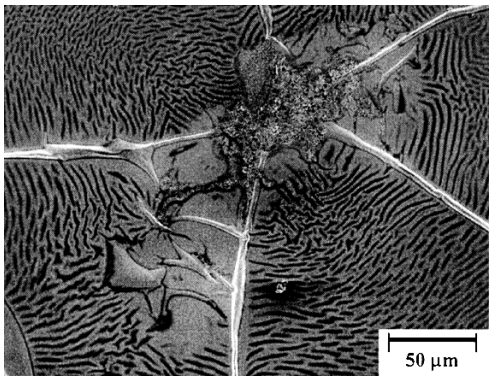

Fig. 5. SEM image of the top Al electrode of the OLEDs.

consequence of the TPD crystallization. In the vicinity of the short, the Al film is likely to be blown up into a starburst opening, or to have formed a fused Al area. The diameter of the electrical short is about 50 μm when measured from Figure 5, much smaller than the value obtained from the temperature and radiant-power images. However, the temperature and radiant-power image systems are able to study the early stage of short formation and to observe the temperature evolution of a working OLED in real time.

The phenomena observed are common to virtually every device that we have tested to date. It is obvious that the thermal breakdown is due to the formation of an electrical short circuit in which a large shunt current passes through a small area. When cutting off the current path to the source isolates the electrical short, the light emission from the undestroyed area will be recovered. Why are OLEDs susceptible to serious electrical short circuiting and thermal breakdown under high voltage stress?

The phenomenon of mild short circuits, sometimes self-healing, is well-known and has been investigated widely.[2,4,8,9] There are several factors including non-planarity at one or both of the organic–electrode interfaces,[4] roughness in the ITO electrode surface, and particulate contamination and inhomogeneity in the organic layer itself.[8,9] These defects induce the electrical short circuits that occur in newly-fabricated devices. After briefly applying a voltage (or several voltages) to new devices, or running a current of several tens of milliamperes through new devices, the short circuit opens, and the device emits light normally. This is not the same as the short circuits investigated and described here. We focus on serious short circuits, followed by thermal breakdown and catastrophic failure, under high-voltage stress (>25 V, or high electrical field $>3\times10^6$ V/cm = 24 V/80 nm).

There are several factors involved in the thermal breakdown and catastrophic failure of OLEDs.[2,5–7,10–29] The degradation of or damage to ITO, diffusion of indium from the ITO electrode into the organic layer,[20–25] and electromigration of the metal cathode[26,27] under the high electric field have been considered to be responsible for serious electrical shorts. The thermal stability of OLEDs dominated by the T_g of the hole transport layer, including the crystallization of the TPD[2,16–19] and the large thermal expansion of TPD associated with its glass transition,[5] is also one of the important factors that govern the stability of OLEDs.[2,10–15]

Under high forward-bias conditions and high electric field, a decomposition reaction at the ITO surface will be expected.[22,25] We also studied the decomposition of ITO under a high electric field in an ultra-high vacuum; these results will be published elsewhere.[24] Anodes with polymeric dopant[28] or doped silicon wafer[29] have improved device efficiency and lifetime, eliminating undesired effects at ITO anodes.

From our results and previous explanations, we propose that the main causes of electrical short-circuiting are decomposition of ITO and electromigration of indium under the electric field in the locations of non-planarity. The detailed process of the thermal breakdown of OLEDs can be described in four steps as follows. 1) The regional high electric field applied to OLEDs induces the decomposition of ITO in locations of non-planarity, resulting in the production of oxygen gas and indium metal. 2) The indium atoms (or ions) diffuse through the organic layer towards to the cathode and the formation of microscopic conduction paths through the organic layer results in a large leakage current. 3) The temperature rise in the defect site as a result of the Joule heating effect enhances the decomposition of ITO and accelerates the electromigration of indium towards the cathode, also spurs crystallization of the TPD. 4) The electrical short circuit, the Joule heat effect, and crystallization of the TPD result jointly in the catastrophic failure or thermal breakdown of the OLEDs.

In summary, real-time temperature measurements on Al/Alq_3/TPD/ITO OLEDs were performed using an infrared thermal imaging and analysis system. Thermal breakdown and surface temperature changes during the whole lifetime of OLEDs have been investigated in detail. From observation, the temperature rise due to the Joule heating effect inside the device is significant and higher than the T_g of TPD under a high forward-bias condition. The electric-field-induced decomposition of ITO and electromigration of indium are responsible for the catastrophic failure, or thermal breakdown, of OLEDs. These results imply that the ITO anode is not very stable under a higher electric field ($>3\times10^6$ V/cm) in Al/Alq_3/TPD/ITO devices. Furthermore, the infrared imaging and analysis system has proved to be a useful and suitable tool for studies on the heat-induced failure of OLEDs. It may also benefit the quality control of OLED production in the future.

Received: April 19, 1999
Final version: July 29, 1999

[1] C. W. Tang, S. A. VanSlyke, *Appl. Phys. Lett.* **1987**, *51*, 913.
[2] J. R. Sheats, H. Antoniadis, M. Hueschen, W. Leonard, J. Miller, R. Moon, D. Roitman, A. Stocking, *Science* **1996**, *273*, 884.
[3] http://www.uniax.com, http://www.cdtltd.co.uk.
[4] P. E. Burrows, V. Bulovic, S. R. Forrest, L. S. Sapochak, D. M. McCarty, M. E. Thompson, *Appl. Phys. Lett.* **1994**, *65*, 2922.

  0935-9648/00/0402-0268 $ 17.50+.50/0

ADVANCED MATERIALS

[5] P. Fenter, F. Schreiber, V. Bulovic, S. R. Forrest, *Chem. Phys. Lett.* **1997**, *277*, 521.
[6] N. Tessler, N. T. Harrison, D. S. Thomas, R. H. Friend, *Appl. Phys. Lett.* **1998**, *73*, 732.
[7] N. Tessler, *Adv. Mater.* **1999**, *11*, 363.
[8] H. Antoniadis, M. R. Hueschen, J. McElvain, J. N. Miller, R. L. Moon, D. B. Roitman, J. R. Sheats, *Polym. Preprint.* **1997**, *38*, 382.
[9] J. McElvain, H. Antoniadis, M. R. Hueschen, J. N. Miller, D. M. Roitman, J. R. Sheats, R. L. Moon, *J. Appl. Phys.* **1996**, *80*, 6002.
[10] S. Tokito, H. Tanaka, K. Noda, A. Okada, Y. Taga, *Polym. Preprint.* **1997**, *38*, 388.
[11] S. Tokito, H. Tanaka, K. Noda, A. Okada, Y. Taga, *Appl. Phys. Lett.* **1996**, *69*, 878.
[12] S. Tokito, H. Tanaka, K. Noda, A. Okada, Y. Taga, *Appl. Phys. Lett.* **1997**, *70*, 1929.
[13] S. A. VanSlyke, C. H. Chen, C. W. Tang, *Appl. Phys. Lett.* **1996**, *69*, 2160.
[14] K. Naito, A. Miura, *J. Phys. Chem.* **1993**, *97*, 6240.
[15] C. Adachi, K. Nagai, N. Tamoto, *Appl. Phys. Lett.* **1995**, *66*, 2679.
[16] M. Fujigira, L. M. Do, C. Ganzorig, A. Koike, T. Kato, *Polym. Preprint.* **1997**, *38*, 380.
[17] E. Han, L. M. Do, Y. Niidome, M. Fujihira, *Thin Solid Films* **1996**, *273*, 202.
[18] E. Han, L. M. Do, Y. Niidome, M. Fujihira, *Chem. Lett.* **1994**, 969.
[19] L. M. Do, E. M. Han, Y. Niidome, M. Fujihira, T. Kanno, S. Yoshida, A. Maeda, A. J. Ikushima, *J. Appl. Phys.* **1994**, *76*, 5118.
[20] A. R. Schlatmann, D. Wilms Floet, A. Hilberer, F. Garten, P. J. M. Smulders, T. M. Klapwijk, G. Hadziioannou, *Appl. Phys. Lett.* **1996**, *69*, 1764.
[21] E. Gautier, A. Lorin, J. M. Nunzi, *Appl. Phys. Lett.* **1996**, *69*, 1071.
[22] C. L. Chao, K. R. Chuang, S. A. Chen, *Appl. Phys. Lett.* **1996**, *69*, 2894.
[23] W. R. Salaneck, J.-L. Brédas, *Adv. Mater.* **1996**, *8*, 48.
[24] J. He, M. Lu, X. Zhou, J. R. Cao, K. L. Wang, L. S. Liao, Z. B. Deng, X. M. Ding, X. Y. Hou, *Thin Solid Films*, in press.
[25] L. S. Liao, X. Y. Miao, X. Zhou, Z. H. Xiong, J. He, Z. B. Deng, X. Y. Hou, *Prog. Nat. Sci.* **1999**, *9*, 84. (in Chinese)
[26] M. Probst, R. Haight, *Appl. Phys. Lett.* **1997**, *70*, 1420.
[27] B. H. Cumpston, K. F. Jensen, *Appl. Phys. Lett.* **1996**, *69*, 3941.
[28] S. A. Carter, M. Angelopoulos, S. Karg, P. J. Brock, J. C. Scott, *Appl. Phys. Lett.* **1997**, *70*, 2067.
[29] X. Zhou, J. He, L. S. Liao, M. Lu, Z. H. Xiong, X. M. Ding, X. Y. Hou, F. G. Tao, C. E. Zhou, S. T. Lee, *Appl. Phys. Lett.* **1999**, *74*, 609.

Patterning of Polymer Light-Emitting Diodes with Soft Lithography

By *Thomas Granlund*,* *Tobias Nyberg*, *Lucimara Stolz Roman*, *Mattias Svensson*, and *Olle Inganäs**

In polymer (opto)electronics, the novel semiconducting polymers need to be patterned using methods suitable for polymers and which do not add great cost to device fabrication. The difficulties encountered with classical photolithography for patterning polymer devices include degradation of the active polymer due to solvents and patterning processes. The patterning of large area structures suitable for displays requires efficient production techniques, where easy printing of structures is feasible. Soft lithography is creating new opportunities for forming microstructures of polymers, ceramics, and metals.[1,2] In this family of techniques, an elastomer stamp is brought into conformal contact with the surface of interest, in order to create a micropatterned surface. New methods of soft lithography for different applications are constantly being developed.[3–5] Microcontact printing,[6] replica molding,[7] and self-assembled monolayers[8] are some methods of soft lithography capable of generating features with lateral dimensions in the sub-micrometer range. Optical systems,[9,10] microanalytical systems,[11] microelectronic devices such as transistors[12–15] and light-emitting diodes,[16] and Bragg reflectors for photo-pumped plastic lasers[17] have been realized with soft lithography. There are several advantages of using soft lithography compared to conventional photolithography: it is less costly, has no optical diffraction limit, allows control of the chemistry of a patterned surface, does not expose the sample to high-energy radiation, and can easily be applied to non-planar surfaces.[18,19] Soft lithography is a gentle process, which therefore is of great interest for patterning sensitive materials such as polymers.

We show here how to use soft lithography to make patterned polymer light-emitting diodes (PLEDs) for passively addressed diode arrays. For this purpose it is sufficient to pattern the anode and cathode layers. The anode layers may be patterned using several techniques, and we present a new method of soft lithography, the lift-up technique.

To prepare our patterned diodes, we need to pattern the anode and the cathode, while the electroluminescent polymer can be a homogeneous global layer deposited by spin-coating. PLED anodes and cathodes were patterned using three different methods of soft lithography: microcontact printing (μCP), lift-up, and micromolding in capillaries (MIMIC). All three methods are shown in Figure 1.

Figure 2a shows the conducting polymer poly(3,4-ethylenedioxythiophene) (PEDOT) and poly(styrene sulfonate) (PSS), which together make up the conducting polymer complex PEDOT–PSS. PEDOT–PSS is known to help inject holes in conjugated polymers, and is therefore widely used. A water dispersion of PEDOT–PSS was used to prepare the patterned anode. The conductivity in a PEDOT–PSS film is ≈1 S/cm using a common thickness of 80–200 nm. We can, however, greatly increase the conductivity by adding other organic compounds to the dispersion, for example, glycerol. The conductivity is then increased by two orders of magnitude after thermally evaporating off the glycerol content in the film. The injection properties seem to be unchanged by this treatment. Fortunately, this blending also makes the polymer more processable and also allows patterning by soft lithography.

We used both μCP and lift-up to pattern anode lines of PEDOT–PSS. The PEDOT–PSS lines produced by μCP (Fig. 1a) showed an edge roughness of 1–2 μm. The width of the smallest lines is 100 μm. Smaller lines can probably

[*] T. Granlund, T. Nyberg, L. Stolz Roman, Dr. O. Inganäs
Department of Physics and Measurement Technology
Laboratory of Applied Physics
Linköping University, S-581 83 (Sweden)
M. Svensson
Department of Organic Chemistry and Polymer Technology
Chalmers University of Technology
S-412 96 Göteborg (Sweden)

  0935-9648/00/0402-0269 $ 17.50+.50/0